

Electro catalytic Oxidation of Reactive Orange 122 in Wastewater by Using Three-Dimensional Electrochemical Reactor (3DER)

¹Mehmet Uğurlu, ²Ali Imran Vaizoğullar*, ¹İlteriş Yılmaz, ¹Müşlih Günbeldek, ³Abdul J. Chaudhary
¹Department of Chemistry, Faculty of Science, Muğla Sıtkı Koçman University, 48000 Muğla/Turkey.
²Vocational School of Healthcare, Med Lab Program, Muğla Sıtkı Koçman University 48000 Muğla/Turkey.
³Institute of Environment, Health and Societies, Brunel University London, UB8 3PH, UK.
aliiimran@mu.edu.tr*

(Received on 15th November 2017, accepted in revised form 6th April 2018)

Summary: In the present study, electrocatalytic treatment of Orange 122 in wastewater was studied by using a three-dimensional electrochemical reactor (3DER). Firstly, TiO₂/AC, V₂O₅/TiO₂/AC and WO₃/TiO₂/AC (over activated carbon) catalysts were prepared by a sol-gel method in aqueous solution. The process optimisation was carried out by investigating the effects of time, voltage, suspension's pH, dye concentration, the amount of supporting electrolyte (NaCl) and the type of catalysts. Optimum values for these parameters were found as 120 min., 15 V, 6.5, 250 mgL⁻¹ and 800 mgL⁻¹ respectively. The results obtained show that after 30 minutes only 30% colour was removed in the absence of activated carbon and this value increased to 60% in the presence of activated carbon. However, the percentage removal increased to 98% in the presence of all three catalytic materials under the same experimental conditions. In addition, for all three catalysts, the pseudo-first-order rate constants were obtained and the values were found to be between $1.12 \times 10^{-2} \text{ min}^{-1}$ and $3.97 \times 10^{-2} \text{ min}^{-1}$. The high removal efficiency of this system is attributed to the synergistic combination of adsorption, electrocatalytic and electrochemical oxidations occurring simultaneously during the oxidation process.

Keywords: Active Carbon, Reactive Orange 122, TiO₂, V₂O₅, WO₃, Electrocatalytic.

Introduction

Currently, there are many industries, for example, food, textile, paper and cellulose, chemical, oil, coal mines, metal finishing, and synthetic rubber/plastic which produce wastewater containing different types of both inorganic and organic pollutants. Textile industry has served as a source of income for many developed and developing countries. The amount of money made in the textile industry runs into billions of US dollars due to the high demand by growing consumers in the clothing market. Major textile producers such as China, US, EU, India, Pakistan, Bangladesh and Turkey have increased production over the past many years. However, the discharge of synthetic textile dyes from textile industries into the aquatic ecosystem poses a threat to its habitants and human health [1].

Dyes presences in wastewaters can cause very significant pollution, even at very low concentrations [2, 3]. Synthetic dyes, present in textile wastewater streams, along with other chemical pollutants can also reduce the light penetration through the water's surface [4]. Textile dyes are relatively resistant to microbial degradation due to their complicated structures [5]. Consequently, it is extremely importance to treat the textile wastewaters in order to remove both dyes and other organic pollutants. The available methods can be categorised

as physical, chemical and biological [6]. Some of these methods are based on adsorption and oxidation, carried out by using Fenton's reagent [7], ozone [8], processes [9, 10]. Many dyes samples used in the industry are resistant to external influences and may be resistant to light and oxidation [11].

The use of different types of electrochemical technologies has many advantages such as high efficiency, environmental compatibility and easy operation [12, 13]. However, in practical applications, the use of the system may be limited due to the low current efficiency and mass transfer constraints due to the formation of diffusion layer. To improve and solve this problem, it is possible to create microelectrodes loaded with an external electric field, increasing the specific surface area of the electrode and increasing the electrolytic activity [14].

As a particle electrode carrier, granulated activated carbon (GAC) is the most widely used material for high specific surface area, good conductivity and low cost [15]. However, it has also been reported that the GAC exhibits a poor capacity for electrochemical oxidation. The solution to this problem is possible to develop the electrocatalytic process by loading the appropriate catalysts into the GAC [16]. TiO₂-photoelectrolysis can be used for the

*To whom all correspondence should be addressed.

degradation of organic pollutants, such as dyestuffs and phenols, which are toxic and non-biodegradable in wastewater effluent streams. TiO_2 is a semiconductor material with excellent catalytic activity and is highly preferred, especially in photocatalytic reactions. Recently, TiO_2 has been reported to have a synergistic contribution to the oxidation reaction without an external light source [17]. However, there are still a limited number of studies related to these issues and therefore, there is a need investigate and define the roles of TiO_2 in electrocatalytic oxidation process.

The main objectives of the work described in this manuscript are: (a) to investigate the feasibility of using TiO_2/AC , $\text{V}_2\text{O}_5/\text{TiO}_2/\text{AC}$ and $\text{W}_2\text{O}_5/\text{TiO}_2/\text{AC}$ as particle electrodes in three dimensional electrochemical reactor (3DER) for the degradation of reactive orange 122 (RO122) and; (b) optimizing parameters (process time, voltage, pH, salt and dye concentration) affecting electrocatalytic oxidation of RO122;

Experimental

Chemicals: Activated carbon, and $(\text{NH}_4)_{10}\text{H}_2(\text{W}_3\text{O}_7)_6$ (Ammonium tungstate) 98 % pure were supplied by Sigma Aldrich; Ti $(\text{OCH}(\text{CH}_3)_2)_4$ (Titanium tetraisopropoxide) 98% pure and NH_4VO_3 (Ammonium monovanadate) 99 % pure were supplied by Merck.

Devices: WiseStir MSH 20A model heating stirrer for mixing operations, Binder brand Etöv oven for drying operations, the Nüve brand muffle furnace, MF 140 model, was used for calcination, Pasco brand SF9584A model power supply for electrocatalytic oxidation experiments, for spectrophotometric measurements, Hach Lange Dr 2800 spectrophotometer, WTW pH330i digital pH meter was used for pH measurement operations. JEOL brand JEM 2100F HRTEM model TEM (Transmission Electron Microscope), JEOL brand JSM-7600F model SEM (Scanning Electron Microscope) and Rigaku brand SmartLab model XRD (X-Ray Diffractometer) were used for surface characterisation.

Synthesis of particles

In this study, TiO_2/AC , $\text{V}_2\text{O}_5/\text{TiO}_2/\text{AC}$ and $\text{W}_2\text{O}_5/\text{TiO}_2/\text{AC}$ catalysts were prepared by loading V_2O_5 and W_2O_5 , separately and together by using TiO_2 as semi-conductor material on the surface of activated carbon (AC) materials.

Synthesis of TiO_2/AC particles

Initially, 500 ml of a solution containing 30% isopropyl alcohol and 100 ml of titanium isopropoxide was prepared. An aliquot of 50 ml of this solution was added over 30 g of AC sample and mixed at constant temperature (25°C). This mixture was first dried in a vacuum oven at 100°C for 2 hours and then left at room temperature. The impregnation process using a 50 ml of solution was repeated 4 times under the same conditions and calcined for one hour at each temperature of 300°C , 400°C and 500°C gradually. After this process, the sample was cooled in a desiccator and kept in dark.

Synthesis of $\text{V}_2\text{O}_5/\text{TiO}_2/\text{AC}$ and $\text{W}_2\text{O}_5/\text{TiO}_2/\text{AC}$ Particles

In this study, 120 ml ethanol and 20 ml tetra-n-butyl titanate were mixed and then 10 ml acetic acid, 2 ml distilled water and a few drops of acetone were added and stirred for 3 hours (solution A). After that, 8-20 mesh AC was activated with nitric acid, washed with distilled water and left for drying. Acid activated carbon was then stirred for three hours with the previously prepared solution A. After the completion of the reaction, dropwise addition of $(\text{NH}_4)_{10}\text{H}_2(\text{W}_3\text{O}_7)_6$ solution was carried under constant temperature to prepare $\text{TiO}_2/\text{W}_2\text{O}_5/\text{AC}$ particles. Prepared particles were filtered and dried at 100°C for 3 hours. Dried samples were thermally activated at 300, 400 and 500°C each for one hour. Same procedure was repeated to prepare $\text{TiO}_2/\text{V}_2\text{O}_5/\text{AC}$ particles but NH_4VO_3 solution was used instead of $(\text{NH}_4)_{10}\text{H}_2(\text{W}_3\text{O}_7)_6$. After these processes, the samples were cooled in a desiccator and kept in a light-free condition.

Electrocatalytic Experiments

In all electro catalytic experimental, TiO_2/AC , $\text{V}_2\text{O}_5/\text{TiO}_2/\text{AC}$ and $\text{W}_2\text{O}_5/\text{TiO}_2/\text{AC}$ materials were used as a catalytic agent. Reactive Orange 122 (RO122) dye was used as a source of chemical contaminant and its chemical structure is shown in Fig 1. The electrolytic system consists of round glass of 500 ml capacity containing three dimensional graphite electrodes as shown in Fig 2. The anode and cathode (feeder electrodes) were situated 5.0 cm apart from each other. Stirring was done by using a magnetic stirrer (50 rpm). Compressed air was sparged into the bed electrodes from the bottom of the reactor.

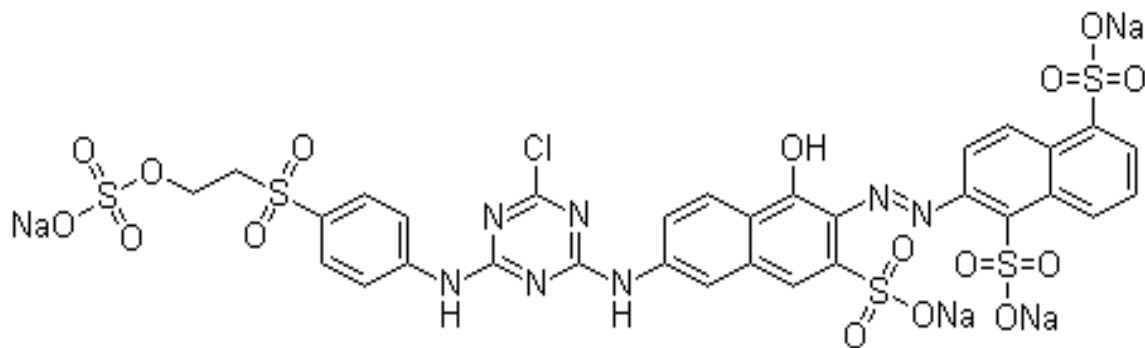


Fig. 1: Chemical structure of textile dye RO 122, λ_{\max} : 488 nm; solubility in water: 75gdm⁻³; degree of purity: 80-85 %.

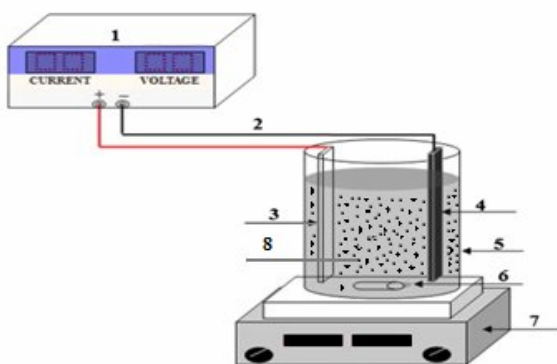


Fig.2: Experimental 3D system for the electrocatalytic treatment of real printing wastewater (1. DC power supply, 2. copper wire, 3. anode, 4. cathode, 5. electrolysis reactor, 6. magnetic bar, 7. electromagnetic stirrer and 8. Catalysts (particle electrode))

For process optimisation, the effect of parameters such as; initial pH, type of catalysts, voltage, wastewater concentration, and the amount of table salt as supporting electrolyte were investigated. Cell voltage was measured digitally by using power supply. At the end of experiments, the treated solution was filtered and then colour changes were measured before and after electrolysis by using a spectrophotometer.

Determination of Colour Change

To determine the λ_{\max} of RO122, the aqueous solution containing a known concentration

of dye was analysed using a UV spectrophotometer. The λ_{\max} of RO122 was found to be at 488 nm. All wastewater samples were analysed at this λ_{\max} value to determine the residual concentration of dyes remaining in aqueous solutions. The percentage removal of RO122 was calculated by using the following formula.

$$\% \text{ colour removal} = \frac{A^0_{\lambda} - A_{\lambda}}{A^0_{\lambda}} \times 100$$

A^0_{λ} : Initial absorbance, A_{λ} : Final absorbance.

Results and Discussion

SEM analyses

The surface morphology of the catalysts prepared as part of this project was investigated using a scanning electron microscopy (SEM) and the SEM images are given in Fig. 3(a, b and c). The SEM micrograph of AC, at the higher magnification (Fig. 3a), clearly show that the AC structure has porous morphology. The SEM images of TiO₂/V₂O₅ and TiO₂/W₂O₅ doped AC samples are given in Fig. 3b and 3c. As seen from these Figs, TiO₂/V₂O₅ and TiO₂/W₂O₅ were attached to the AC surface. The proof of this adhesion was demonstrated by Energy Dispersive X-ray Spectroscopy (EDS) and compositional element rates obtained by EDS (Table-1).

Table-1: EDS results of the three catalytic samples.

	Element (Weight %)									
	C	O	Ti	V	W	Mg	Ca	Si	P	Totals
AC	86.71	11.00	-	-	-	0.84	0.82	0.46	0.32	100.00
V ₂ O ₅ /TiO ₂ /AC	65.47	21.37	12.10	1.07	-	-	-	-	-	100.00
WO ₃ /TiO ₂ /AC	71.66	20.75	6.39	-	1.21	-	-	-	-	100.00

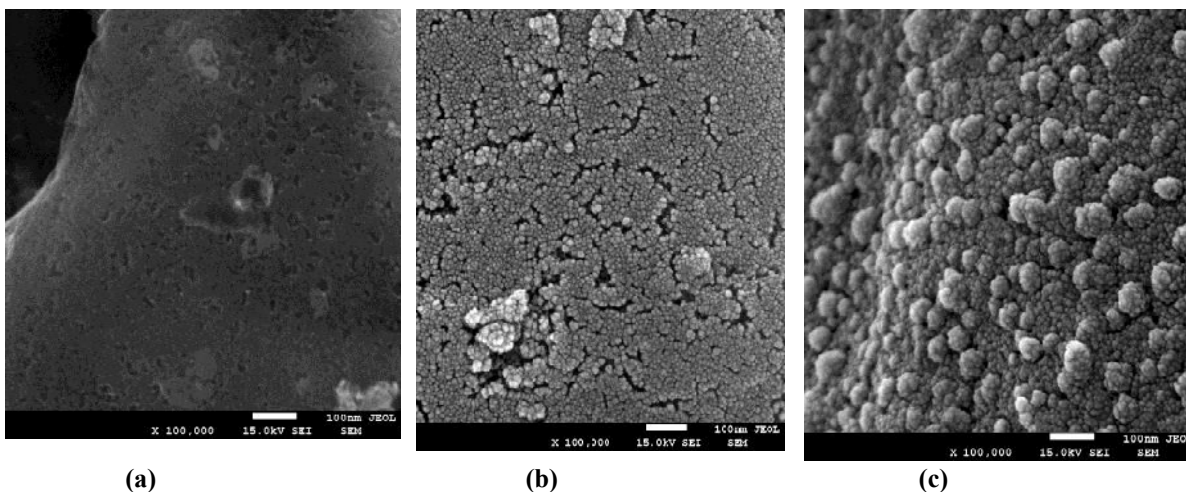


Fig. 3: SEM images belonging to Activated carbon (a), $V_2O_5/TiO_2/AC$ (b) and $WO_3/TiO_2/AC$ (c).

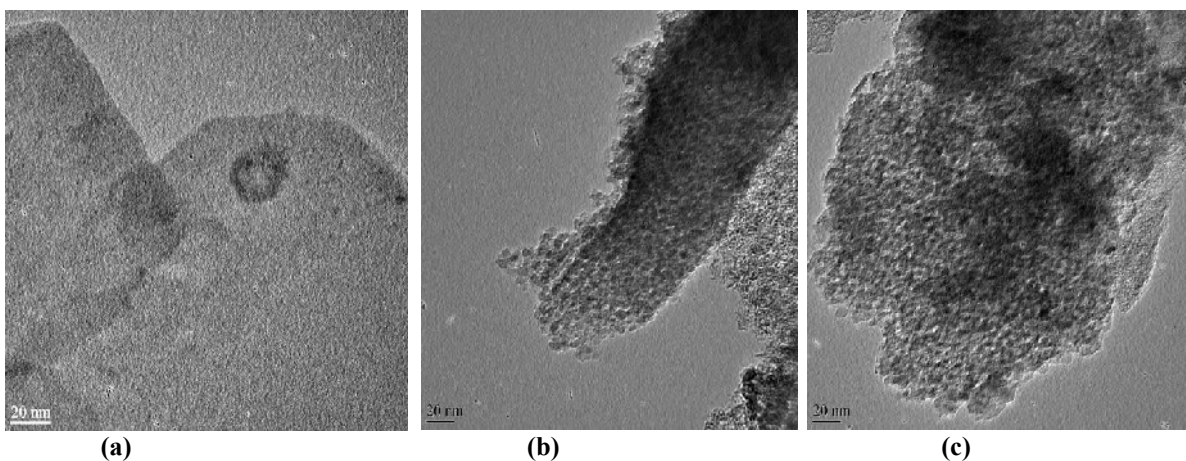


Fig., 4: TEM images belonging to AC (a), $V_2O_5/TiO_2/AC$ (b) and $WO_3/TiO_2/AC$ (c).

TEM analyses

The samples were also analysed using a transmission electron microscopy (TEM) for investigating the morphology of the prepared catalysts. Fig. 4 (a, b, c) shows the images with increasing magnifications from the samples. Fig. 4a shows the typical TEM micrograph of the amorphous AC. The TEM images of TiO_2/V_2O_5 and TiO_2/W_2O_5 doped AC samples are presented in Fig. 4b and 4c. As seen in the Fig.4b and 4c, TiO_2/V_2O_5 and

TiO_2/W_2O_5 were attached to the AC as with SEM results.

XRD analysis

Fig. 5 shows the XRD patterns of TiO_2/AC (a), $V_2O_5/TiO_2/AC$ (b) and $WO_3/TiO_2/AC$ (c) amorphous and crystal structures. According to Fig. 5, the X-ray patterns confirm that activated carbon samples were amorphous and TiO_2/V_2O_5 and TiO_2/W_2O_5 doped samples have crystal diffractions peaks.

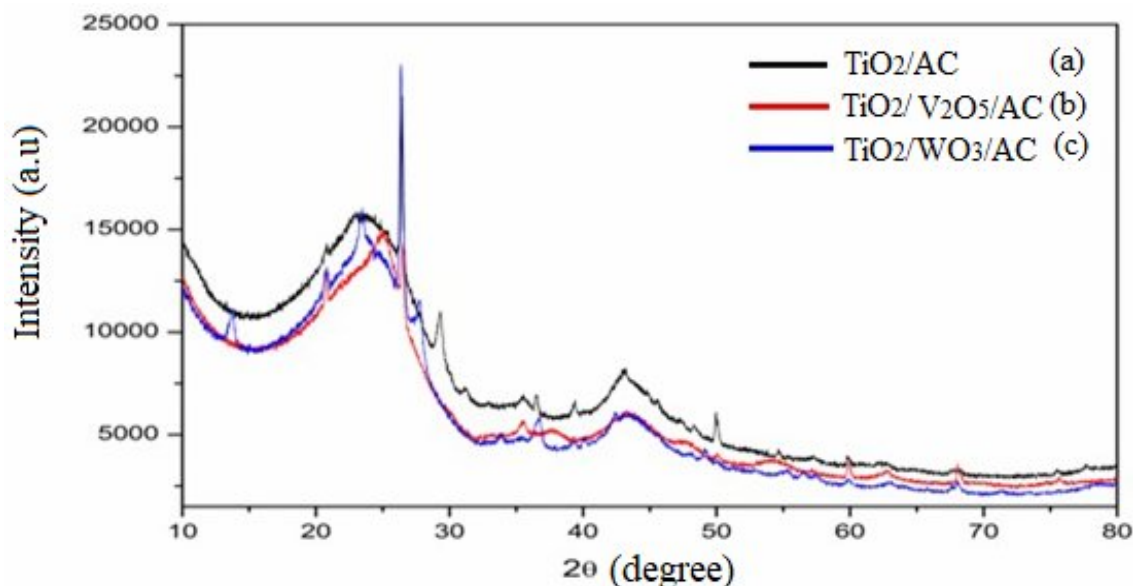


Fig. 5: XRD spectra belonging to TiO_2/AC , $\text{TiO}_2/\text{V}_2\text{O}_5/\text{AC}$ and $\text{TiO}_2/\text{WO}_3/\text{AC}$

FTIR Analysis

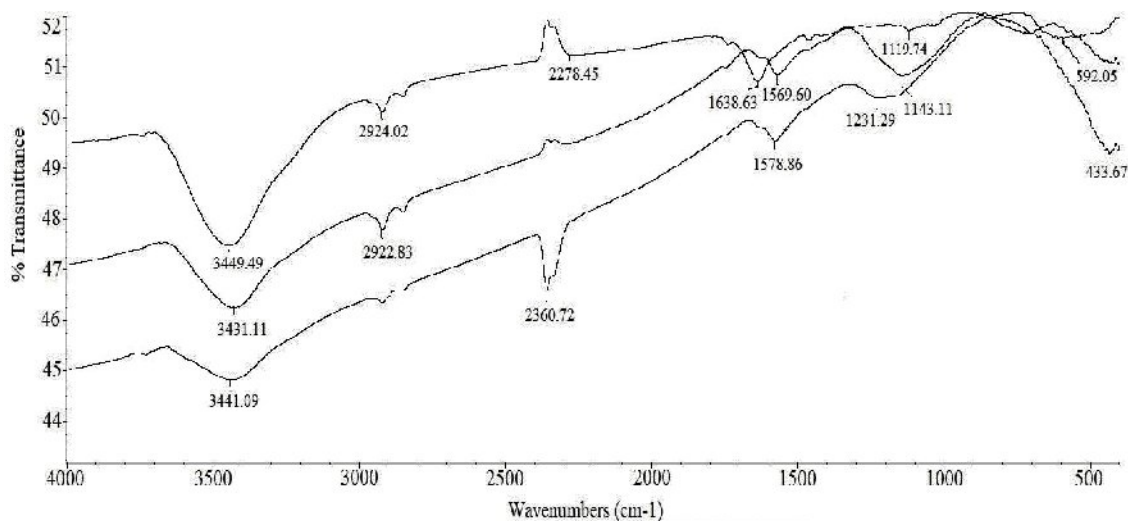


Fig. 6: FTIR spectra belonging to TiO_2/AC (a), $\text{V}_2\text{O}_5/\text{TiO}_2/\text{AC}$ (b) and $\text{WO}_3/\text{TiO}_2/\text{AC}$ (c).

When compared, both AC and TiO_2/AC spectra showed stretching vibration at 3440 cm^{-1} related to $-\text{OH}$. $\text{C}-\text{H}$ stretching was also observed at 2923 cm^{-1} related to $-\text{CH}_2$. Band height and broadness reflects that these groups did not change after the application of TiO_2 . The band at 1575 cm^{-1} disappeared that was related to aromatic $\text{C}=\text{C}$ and a new band appeared at 1638 cm^{-1} related to titanium carboxylate. Disappearance of $\text{C}=\text{C}$ related band and appearance of TiO_2 bands proves the impregnation of TiO_2 particles on the surface of AC (Fig. 6a).

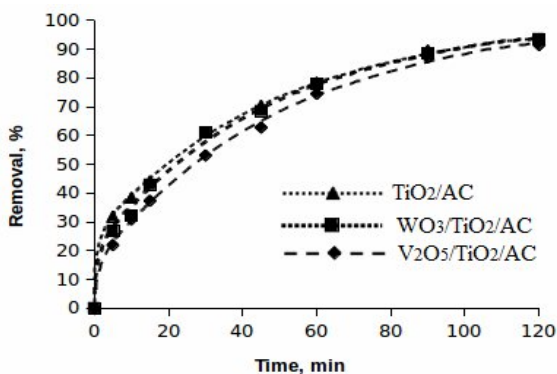
Hydroxyl band on the surface of $\text{V}_2\text{O}_5/\text{TiO}_2/\text{AC}$ decreased and shifted to 3431 cm^{-1} was also observed. It was different from WO_3 as $-\text{CH}_2$ bands did not disappear that means they were unaffected, only $-\text{OH}$ groups were involved in reaction. Similar to WO_3 connectivity, bands at 1638 cm^{-1} related to titanium carboxylate disappeared. Similarly, the $\text{C}=\text{C}$ band at 1575 cm^{-1} shifted to 1569 cm^{-1} after reaction with V_2O_5 . The $\text{C}-\text{O}$ band at 1156 cm^{-1} in pure AC also shifted to 1143 cm^{-1} after the removal of titanium carboxylate and reaction with V_2O_5 (Fig.

6b). After comparing the spectrum of $\text{WO}_3/\text{TiO}_2/\text{AC}$, the band of $-\text{OH}$ shifted from 3440 cm^{-1} to 3441 cm^{-1} and area under the peak is also decreased in addition to the disappearance of $-\text{CH}_2$ band at 2924 cm^{-1} after the addition of WO_3 (Fig. 6c). Therefore, it can be believed that WO_3 affected these groups. Separately, the band related to titanium carboxylate after the addition of TiO_2 disappeared after heating and a small peak was observed at 1578 cm^{-1} . Another band appeared at 1231 cm^{-1} that is related to $\text{W}=\text{O}$. It proved the addition of WO_3 .

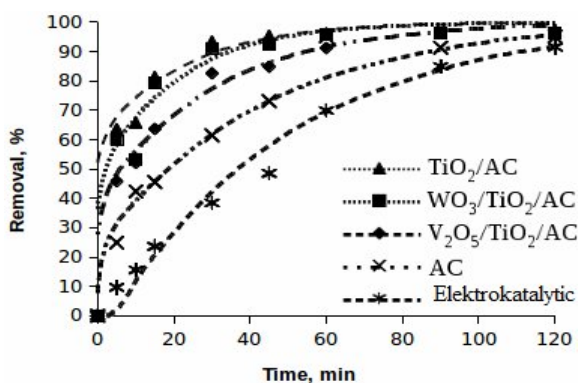
Effect of Experimental Parameters

The Effect of Salt Concentration

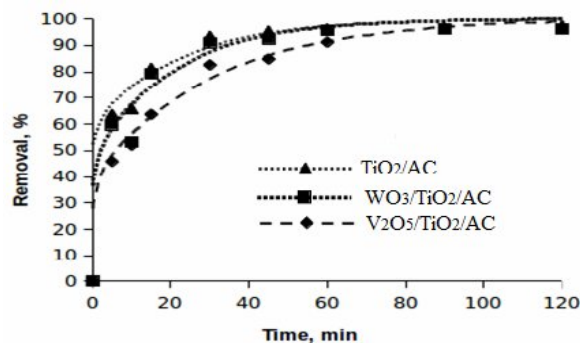
The salt concentration in the electrochemical reactions is important because it acts as a supporting electrolyte and determines the electrolytic current. The increase in electrical current intensity can improve not only the degradation of organic pollutants present in wastewater streams but also some side reaction such as producing H_2 at cathode. The results are shown in Fig 7 at varying NaCl amounts for colour removal.



(a)



(b)



(c)

Fig 7: Changes in colour removal rates over time depending on catalyst and salt concentrations. (a: 0.4 gL^{-1} , b: 0.8 gL^{-1} and c: 1.6 gL^{-1}) (voltage: 15V , pH: 6.5 and concentration: 250 mg/L).

The data in Fig. 7 show that the percentage removal of colour depends on the concentration of salt used during the reaction. The best removal percentage was obtained when 0.8 g L^{-1} salt was used in all electro catalytic experiments. No advantages in the colour removal were achieved by increasing the salt concentration from 0.8 g L^{-1} to 1.6 g L^{-1} . In addition, it was observed that 90 % colour removal was achieved at the end of 30 minutes, and then this percentage remained constant. The addition of salt (NaCl) would also lead to the decrease in power consumptions because of an increase in conductivity [17, 18] during the degradation process. The main reactions occurring during the anodic oxidation of organic compounds in the presence of NaCl are given below

Anode

Hypochlorite formation:
 $\text{Cl}^- + 2\text{OH}^- \rightarrow \text{OCl}^- + \text{H}_2\text{O} + 2\text{e}^-$

Cathode

Hydrogen evolution:
 $2\text{H}_2\text{O} + 2\text{e}^- \rightarrow \text{H}_2 + 2\text{OH}^-$

Chlorate formation:
 $6\text{ClO}^- + 3\text{H}_2\text{O} \rightarrow 2\text{ClO}_3^- + 4\text{Cl}^- + 6\text{H}^+ + 3/2\text{O}_2 + 6\text{e}^-$

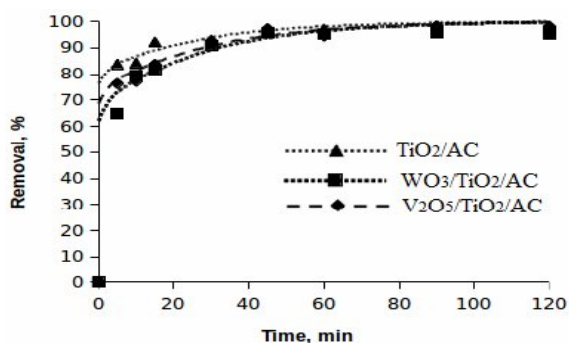
Oxygen evolution:
 $4\text{OH}^- \rightarrow 2\text{H}_2\text{O} + \text{O}_2 + 4\text{e}^-$

Solution and/or near the surface of anode electrode, Indirect oxidation of dye compound and its oxidation intermediate with hypochlorite in electrochemical treatment of dye effluent via chlorine generation is:

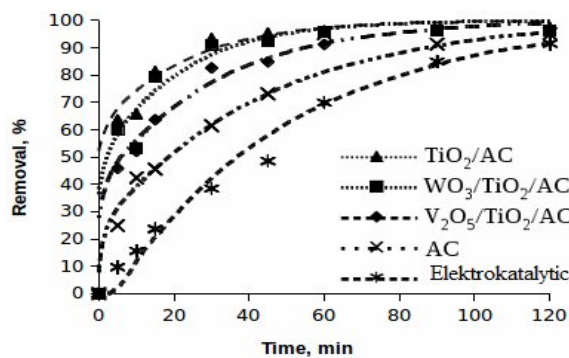


Effect of Dye Concentration

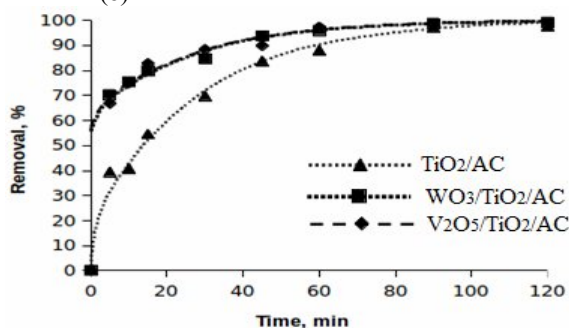
Electro catalytic experiments were carried out using wastewater streams containing three different concentrations (125 mg L⁻¹, 250 mg L⁻¹ and 500 mg L⁻¹) of dye. The percentage removal of colour observed over time depends on the initial concentration of dye present in wastewater streams (Fig. 8).



(a)



(b)



(c)

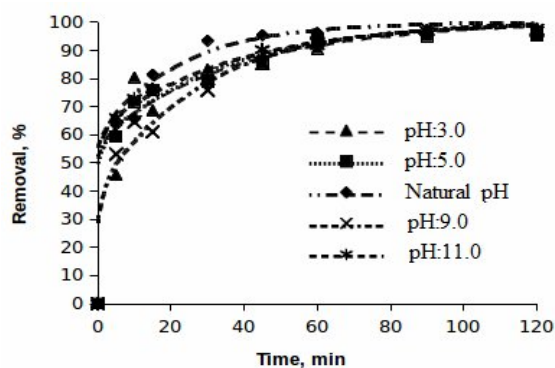
Fig 8: Effect of initial concentrations of the dye on the percentage removal of colour vs time (a: 125 mg L⁻¹, b: 250 mg L⁻¹ and c: 500 mg L⁻¹). (NaCl: 0,8 g L⁻¹, voltage: 15V, pH: 6,5).

The data in Fig. 8 show that the percentage removal of colour increased with time. The percentage removal after 15 minutes was 90% when the dye

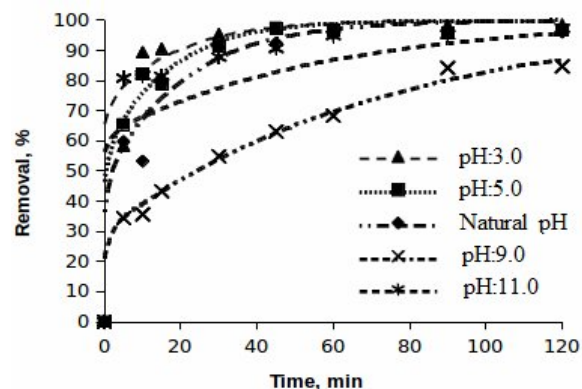
concentration was 125 mg L⁻¹. However, the percentage removal decreased to 80% and 70% when the dye concentration was increased to 250 and 500 mg L⁻¹ respectively. It was also observed that the percentage removal of colour reached to a maximum value of 99% after 120 minutes for all concentrations under different catalytic conditions. At low initial concentrations, it was seen that the electrocatalyst reaction is faster than the diffusion. Too many dye molecules in solution could not be removed completely for the agglomeration of organics and the shortage of reactive oxidative species. It was observed that the percentage removal of colour reached 99% when the dye concentration was 250 mg L⁻¹. In view of these results, the later experiments were carried out using 250 mg L⁻¹ of dye. The results indicate that the RO122 degradation at different initial concentrations ranging from 125 to 500 mg L⁻¹ is in good agreement with the pseudo-first-order kinetics. The rate constant for all catalyst samples are shown in Table-1

pH Effect

The pH of solution in the electrocatalytic reactions taking place on the particle surface is an important parameter. The colour removal for three catalyses was examined at different pH and the obtained results are plotted in Fig. 9.



(a)



(a)

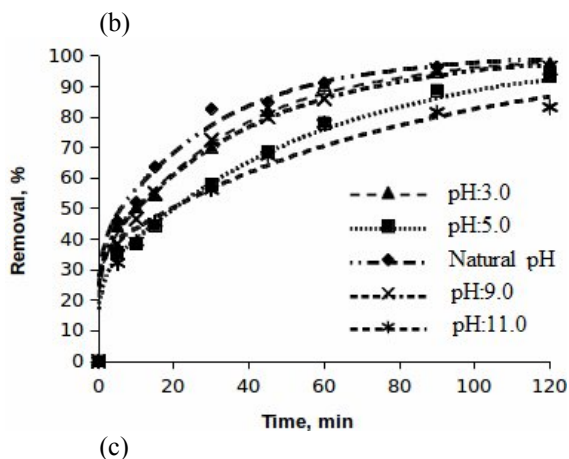


Fig.9: Effect of pH on the percentage removal of colour using (a: TiO_2/AC , b: $\text{WO}_3/\text{TiO}_2/\text{AC}$, c: $\text{V}_2\text{O}_5/\text{TiO}_2/\text{AC}$, solid/liquid: 0.8 gL^{-1} , voltage: 15V , Init.cons.: 250 mgL^{-1}).

The results also showed that the colour removal efficiency reached the highest level at pH: 5.0 and pH: 3.0. It is mainly because that quinoid structure may be more likely to be degraded, and quinoid structure is a main form at the low pH value [19]. In addition, it is well known that the increase of the solution pH is favourable for the occurrence of secondary reaction (oxygen evolution) meaning more energy consumption, which results in decreasing the current efficiency. The data in Fig. 9a show that the optimum pH condition nearly 99% of the original colour was removed after 120 minutes.

Voltage Effect

Electrocatalytic experiments were carried out firstly with carbon electrode and then TiO_2/AC , $\text{WO}_3/\text{TiO}_2/\text{AC}$ and $\text{V}_2\text{O}_5/\text{TiO}_2/\text{AC}$, using the catalysers separately at different voltages (10, 15 and 20 V). The results obtained are plotted in Fig.10 respectively.

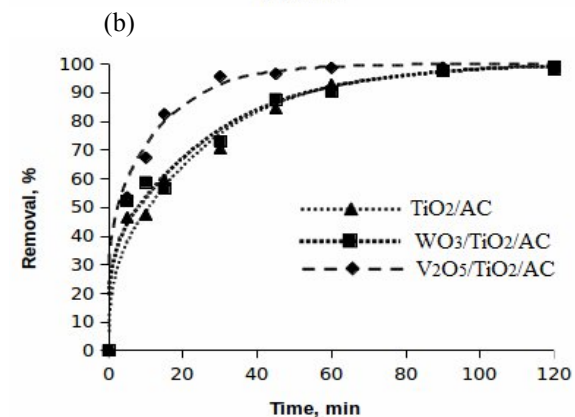
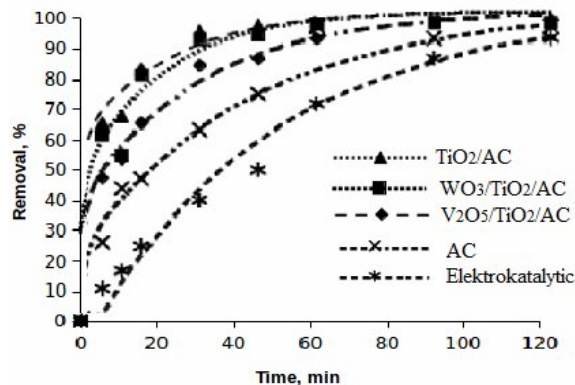
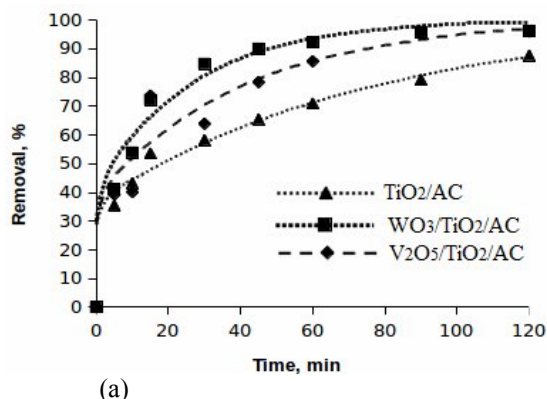


Fig.10: Effect of voltage on the percentage removal of colour vs time (a:10 V, b:15 V, and c:20 V) (NaCl conc: 0.8 gL^{-1} , pH:6.5, Initial dye conc: 250 mgL^{-1})

The results obtained show that 65% colour removal was achieved after the first 5 minutes under the optimum condition of 0.2 g L^{-1} catalyst, natural pH, 0.8 g L^{-1} NaCl and 15 V. This degradation value was increased to 96% after 60 minutes. The highest percentage removal of colour was obtained with TiO_2/AC , closely followed by TiO_2/AC and $\text{WO}_3/\text{TiO}_2/\text{AC}$, $\text{V}_2\text{O}_5/\text{TiO}_2/\text{AC}$. It was also observed that the lowest percentage removal was achieved at 10 V with the use of TiO_2/AC as catalyst. However, higher percentage removal was achieved at the same voltage when $\text{WO}_3/\text{TiO}_2/\text{AC}$ catalyst was used. When the voltage was increased to 20 V then the highest percentage removal was obtained with the use of $\text{V}_2\text{O}_5/\text{TiO}_2/\text{AC}$ catalysts. Overall, the percentage removal increased with increasing the voltage from 10 to 20 V.

Catalytic Mechanism

It has been reported that a higher percentage removal of dyes can be obtained when GAC

supported TiO₂ particle electrode was used instead of using GAC alone for the removal of organic dye (in 3D system) [20]. Based on the experimental results, TiO₂/AC, TiO₂/WO₃/AC and TiO₂/V₂O₅/AC have been demonstrated to possess a much higher electrocatalytic activity for oxidizing organic pollutants than only AC and electrooxidation (as well as the 2D system).

It is well known that the hydroxyl radical ([•]OH) plays an important role in the removal of organic compounds because it is a very powerful oxidizing agent. In the literature study, it has been reported that electrogeneration increase of [•]OH occurs in the aqueous medium when electrical current is applied to GAC material in electrochemical oxidation systems (in 3D system) [21, 22]. In another study, it has been reported that in the removal of paint with [•]OH, H₂O₂ never reacts actively with dye molecules, significant amounts of [•]OH are produced in the presence of AC especially, and the dye molecules can be rapidly oxidized [23].

In the present study; semiconductor materials such as TiO₂, WO₃, V₂O₅, TiO₂ and AC

were used together or separately. The valence and conduction bands of VO₂ and WO₃ are higher than those of TiO₂. Therefore, electrochemical generated electrons in VO₂ and WO₃ are transferred to the conduction band of TiO₂, and photogenerated holes in TiO₂ will be transferred to the valence band of WO₃ and VO₂. The photogenerated electrons and holes are thus highly separated in pore and surface of AC, increasing their catalytic activity. In addition, the larger surface and porous structures of AC would also increase the catalytic activity, because more organics can be adsorbed. When it is thought that all of sentezed, catalyzers are typical “nonactive” electrocatalyst, at this “nonactive” metal oxide electrode (MO_x) over granular activated carbon (GAC) surface, water molecules were easily decomposed to form strong oxidants, such as physisorbed [•]OH, MO_x ([•]OH) which allow nonselective oxidation of organics and may result in complete oxidation of organic carbon to CO₂. As schematic representation describing the possible mechanisms involving the 3D electrocatalytic process is therefore provided in Fig. 11.

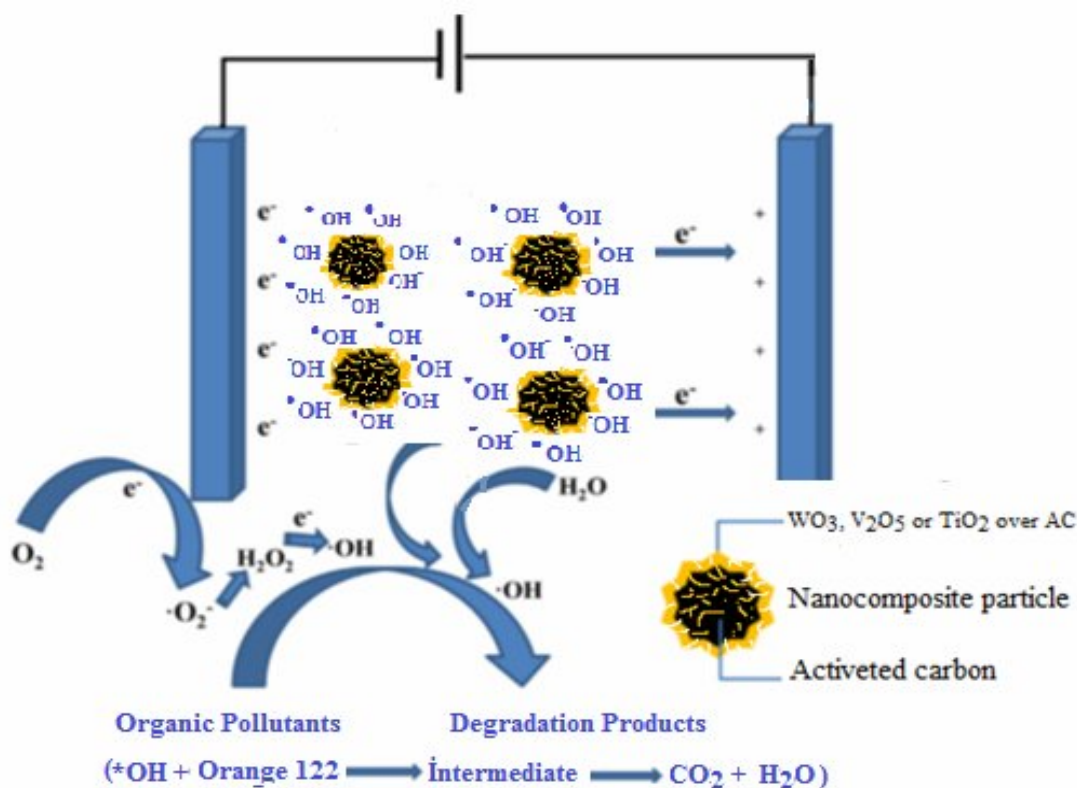


Fig. 11: (A) schematic representation describing the mechanisms of the charge separation and active species generation in a 3D electrocatalytic system

Table-2: k and R² values for Colour removal to different parameters and nanoparticles.

Parameters	TiO ₂ /AC		WO ₃ /TiO ₂ /AC		V ₂ O ₅ /TiO ₂ /AC	
	R ²	k × 10 ⁻² (min ⁻¹)	R ²	k × 10 ⁻² (min ⁻¹)	R ²	k × 10 ⁻² (min ⁻¹)
Salt effect (g L ⁻¹)						
0,4	0,99	2,19	0,99	2,23	0,99	2,05
0,8	0,75	2,77	0,82	2,83	0,92	2,55
1,6	0,78	3,21	0,80	2,63	0,91	3,55
Concentration (mg L ⁻¹)						
125	0,70	2,59	0,78	2,72	0,80	3,21
250	0,75	2,77	0,78	2,69	0,95	2,97
500	0,97	3,26	0,95	3,84	0,88	3,44
Voltage effect (V)						
10	0,86	3,71	0,88	2,72	0,96	2,94
15	0,96	2,89	0,88	3,34	0,96	3,06
20	0,94	1,12	0,99	3,97	0,86	3,87
pH effect						
3	0,92	3,08	0,72	3,05	0,98	3,04
5	0,83	2,32	0,74	2,46	0,99	2,15
6,5	0,75	2,77	0,78	2,72	0,94	2,91
9	0,93	3,08	0,96	1,38	0,97	2,75
11	0,89	2,72	0,79	2,34	0,90	1,45

In the 3D reaction system with WO₃, V₂O₅ or TiO₂ over granule activated carbon used, each particle electrode could act as a micro electrolysis cell. As a result, the 3D electrocatalytic system owns much higher electrode areas than 2D reaction, and the process performance is much improved [24-26]. Overall, in the 3D photoelectrocatalytic system, the high degradation efficiency of RO122 should be explained to the synergistic effect of activated carbon adsorption, electrocatalytic and electrochemical oxidation. Another advantage of the granular particle in practical application, the composite material could still be easily recovered from the bulk solution by using filter apparatus after the electrocatalytic reaction.

Photo degradation kinetics.

The degradation kinetics of wastewater by using three catalysts were evaluated using the linearized form of pseudo first- order rate

$$\ln(C_t/C_o) = -kt \quad (5)$$

where C_o , C_t , t and k are the initial concentration (mg L⁻¹), the concentration (mgL⁻¹) at time t , exposure time and the first-order rate kinetics, respectively. Table-2 shows that the degradation process follows the pseudo first-order rate kinetics as evidenced from the regression (r^2) analysis that is greater than 0.70. The higher rate constant achieved using TiO₂/AC can be attributed to the combined effects of adsorption of organic molecule over catalyst surface followed by oxidation using the generated hydroxyl radical and direct attack of photo generated holes [27]

Conclusions

In this study, the electrocatalytic degradation of RO122 was investigated by using graphite electrode and also as particle electrodes. The removal of RO122 in the three-dimensional electrode system was mainly dependent on the oxidation by active substances (O[•], etc.). The efficiencies of nanocomposite materials were examined in the operation condition., optimum values were found as reaction time; 120 min., voltage; 15 V, solution pH; 6.5; initial concentration; 250 mg L⁻¹ and NaCl concentration; 0.8 g L⁻¹. The kinetics analysis results indicated that the degradation of RO122 in systems followed pseudo first-order kinetics. For all catalysts, the pseudo-first-order rate constants were obtained among $1.12 \times 10^{-2} \text{ min}^{-1}$ and $3.87 \times 10^{-2} \text{ min}^{-1}$.

The dye degradation mechanism in 3D system is very complex, and in general two different mechanisms are considered to be responsible for dye degradation: (1) direct oxidation of dye molecules by the direct electron transfer reaction; (2) indirect oxidation by the aqueous oxidants such as hydroxyl radicals and hydrogen peroxide

The above results validated 3D electrolysis as a promising alternative method for removing dyes from secondary effluents in pre-treatment or advanced treatment applications. The practical implementation of this technology is encouraged, especially in locations where renewable or self-produced energy is available.

Moreover, the necessity to analyse and identify the formation of different intermediate products using modern analytical techniques equipped with identification library is needed. It

would also be useful to identify the structure of these intermediate products to fully understand the degradation mechanism during the electrocatalytic oxidation process using HPLC, gas chromatography, NMR and other analytical techniques in further studies.

Acknowledgements

This study was financially supported as a project (15/041) by Research Project Coordination Unit, Muğla Sıtkı Koçman University. The authors wish to thank Muğla Sıtkı Koçman University for XRD, FTIR, SEM and TEM analyses.

References

1. T. Uruj, Y. Azra and H. K. Umair, Phytoremediation: Potential flora for synthetic dyestuff metabolism, *J. King. Saud. Univ. Sci.*, **28**,119 (2016).
2. P. Nigam, G. Armour, I. M. Banat, D. Singh, and R. Marchant, Physical removal of textile dyes from effluents and solid-state fermentation of dye-adsorbed agricultural residues, *Bioresource Technol.*, **72**, 219 (2000).
3. A. Gürses, M. Yalçın and Ç. Doğar, Electrocoagulation of some Reactive Electrochemical Variables, *Waste Manage.*, **22**, 491 (2002).
4. A. Gürses, M. Yalçın and Ç. Doğar, Investigation on settling velocities of aluminium. 500 hydroxide-dye flocs. *Fresen. Environ. Bull*, **12**,16 (2003).
5. O. Yesilada, S. Cing and D. Asma, Decolourisation of textile dye Astrazon Red FBL by *Funalia trogii* pellets, *Bioresource Technol.*, **81**, 155 (2002)
6. T. Robinson, B. Chandran and P. Nigam, Effect of pre-treatments of three waste residues, wheat straw, corncobs and barley husks on dye adsorption, *Bioresource Technol.*,**85**(2),119 (2002).
7. D. Pak and W. Chang, Decolorizing dye waste water with low temperature catalytic oxidation. *Wa. Sci. Technol.*, **40**:115 (1999)
8. F. Dinçer, M. H. Karaoğlu, M. Uğurlu, and Aİ. Vaizoğullar. Ozonation of Reactive Orange 122 Using La³⁺-Doped WO₃/TiO₂/Sep Photocatalyst., *Ozone-Sci. Eng.*,**38** (4):291 (2016)
9. A. Gürses, S. Karaca, Ç. Doğar, M. Açıkyıldız, R. Bayra, and M. Yalçın. Determination of adsorptive properties of clay/water system: methylene blue sorption. *J Colloid Interf Sci*, **269** (2):310 (2004).
10. F. Akbal, Adsorption of basic dyes from aqueous solution onto pumice powder *J. Colloid Interf. Sci.*, **286** (2) 455 (2005).
11. X. Wu, X. Yang, D. Wu and R. Fu, Feasibility study of using carbon aero gel as particle electrodes for decoloration of RBRX dye solution in a three dimensional electrode reactor, *Chem. Eng. J.* **138**, 47–54(2008).
12. S. Liu, X. Feng, F. Gu, X. Li and Y. Wang, Sequential reduction/oxidation of azo dyes in a three-dimensional biofilm electrode reactor, *Chemosphere*, **186**, 287 (2017).
13. J. Radjenovic, D. L. Sedlak, Challenges and opportunities for electrochemical processes as next-generation technologies for the treatment of contaminated water, *Environ. Sci. Technol.*, **49**, 11292 (2015).
14. X. Y. Li, Y. Wu, W. Zhu, F.Q. Xue, Y. Qian, and C.W. Wang, Enhanced electrochemical oxidation of synthetic dyeing wastewater using SnO₂-Sb-doped TiO₂-coated granular activated carbon electrodes with high hydroxyl radical yields, *Electrochim. Acta.*, **220**, 276 (2016).
15. H. Z. Zhao, Y. Sun, L. N. and Xu, J. R., Ni Removal of Acid Orange 7 in simulated wastewater using a three-dimensional electrode reactor: Removal mechanisms and dye degradation pathway, *Chemosphere*, **78**, 46 (2010).
16. J. W. Shi, J. T. Zheng and X. J. Ji TiO₂-SiO₂/activated carbon fibers photocatalyst: preparation, characterization, and photocatalytic activity, *Environ. Eng. Sci.*, **27**, 923 (2010).
17. X. Yan, L. Juan, X. Jin-Ping, C. Lei Feng, Y. Fei Shi, and J. Ji, TiO₂-SiO₂/GAC particles for enhanced electrocatalytic removal of acid orange 7 (AO7) dyeing wastewater in a three-dimensional electrochemical reactor, *Separation and Purification Technology*, **187**, 303 (2017).
18. M. S. Morsia, A. A. Al-Sarawy, and W. A. Shehab El-Dein, Electrochemical degradation of some organic dyes by electrochemical oxidation on a Pb/PbO₂ electrode, *Desalination Water Treat.*, **26**:301 (2011)
19. AI. Vaizogullar, M. Ugurlu, A. Ayyildiz, SI Yilmaz, and A. J Chaudhary, TiO₂, WO₃, and V₂O₅, Supported On Activated Carbon: Preparation, Structural and Catalytic Behaviour In Photocatalytic Treatment Of Phenol and Lignin From Olive Mill Wastewater, *Fresen Environ Bull.*, **26**, 3529 (2017).
20. Y. Xiu, X. Juan, C. Jin-Ping, F. Lei, S. Ya-Fei, J. Jing, TiO₂-SiO₂/GAC particles for enhanced electrocatalytic removal of acid orange 7 (AO7) dyeing wastewater in a three-dimensional

- electrochemical reactor, *Separation and Purification Technology*, **187**, 310 (2017).
21. H. Sun Z. Liu, Y. Wang, and Y. Li, Electrochemical in situ regeneration of granular activated carbon using a three-dimensional reactor, *J. Environ. Sci.*, **25**, 77 (2013).
 22. Z. Kang, T. Letian, T. Yufei and C. Xi, Titanium oxide/vanadium oxide composite nanofibers formed by electrospinning and dipping in vanadium sol, *Ceramics International*, **40**, 15335 (2014).
 23. S. Liu, Y. Wang, B. Wang, J. Huang, S. Deng and G. Yu., Regeneration of Rhodamine B saturated activated carbon by an electro-peroxone process, *Journal of Cleaner Production*, **168**, 594 (2017).
 24. C. Zhang, Y. Jiang, Y Li. Z. Hu, L. Zhou and M. Zhou, Three-dimensional electrochemical process for wastewater treatment: A general review, *Chem. Eng. J.*, **228**: 455 (2013).
 25. J. Song, X.Wang, J. Huang, J. Ma, X. Wang, H. Wang, R. Ma, P. Xia, and J. Zhao, High performance of N-doped TiO₂-magnetic activated carbon composites under visible light illumination: Synthesis and application in three-dimensional photoelectrochemical process, *Electrochim. Acta.*, **222**, 1 (2016).
 26. S. Liu, H. Song, S. Wei, Q. Liu, X. Li and X. Qian, Effect of direct electrical stimulation on decolourization and degradation of azo dye reactive brilliant red X-3B in biofilm-electrode reactors, *Biochem. Eng. J.*, **93**, 294 (2015).
 27. M. Uğurlu and H. Karaoğlu, Removal of some compounds from bleached kraft mill effluent by UV oxidation in the presence of hydrogen peroxide utilizing TiO₂ as photocatalyst, *Environ. Sci. Pollut. Res.*, **16**, 265 (2009).